A Shape Memory Polymer with Improved Shape Recovery*

Changdeng Liu[1] and Patrick T. Mather[2]
[1]Chemical Engineering, University of Connecticut
[2]Institute of Material Science, University of Connecticut

ABSTRACT

Thermally actuated shape memory polymers (SMPs) interest, both academically and industrially, due to their ability to memorize a permanent shape that is set during processing and a temporary shape that is later programmed by manipulation above a critical temperature, either T_g or T_m. However, the thermal triggering process for SMPs is usually retarded compared to that of shape memory alloys, because the thermal conductivity of polymers is much lower (<0.30 W/m·K). In the present study, we incorporated a highly thermal conducting filler into a shape memory matrix to increase its thermal conductivity and therefore, shorten the heat transfer progress. A mathematical was worked out that quantitatively relates the material's thermal conductivity with the heat transfer time, τ, also defined as a shape memory induction time. The model fit nicely with our experimental data. In addition, mechanical reinforcement was observed with the addition of this rigid thermal conducting filler.

INTRODUCTION

Research and application development in the area of shape memory polymers (SMPs) have been a fast growing topic both academically and industrially due to the advantages of the memorizing function that enable ordinarily static plastics to be used as smart materials and to a broad variability of thermomechanical properties. For the majority of SMPs, shape 'fixing' and recovery are thermally triggered. Consequently, both the fixing and recovery events for most SMPs involve the transfer of heat from an external source to the SMP. Compared with its cousin, shape memory alloys (SMAs), which intrinsically have a high thermal conductivity, the thermal conductivity of polymer is relatively low[1], which greatly reduced the shape fixing and shape recovery process, especially for bulky samples. Therefore, besides the relaxation times and the crystallization kinetics of these materials, heat transfer during the thermally indeed actuation process plays a very important role in controlling the shape fixing and shape recovery speed.

In a previous report, we succeeded in increasing (doubling) the thermal conductivity of a shape memory rubber by incorporation of a highly thermal conducting filler [2]. The mechanical properties of the filler modified composites also increased both in the crystalline and rubbery regions of the dynamical mechanical analysis (DMA) profiles, without noticeably affecting the transition temperature and transition sharpness.

Going beyond the effect of such a filler on thermal conductivity alone, the present paper focuses on the evolution of spatial temperature profiles with time when being heated, the effect of thermal conductivity on such profiles, and finally on the shape recovery speed for a particular material system.

*Adapted from Chapter 6 of Changdeng Liu's PhD Dissertation, University of Connecticut (2004).

THEORY

To investigate the effects of the heat transfer on the temperature profile within the bulk samples when immersed in a hot media, we first assume that the shape memory polymer is an infinite slab so that the heat transfer is one-dimensional through the thickness of the samples. Derived from an unsteady state heat conductivity equation, when such an infinite slab with temperature T_0 is immersed into a hot bath with temperature T_1, the temperature profile of the slab with thickness of $2b$ can be expressed to arbitrary precision as [3,4]:

$$\frac{T_1 - T(y,t)}{T_1 - T_0} = 2\sum_{n=0}^{\infty} \frac{(-1)^n}{(n+\frac{1}{2})\pi} e^{-(n+\frac{1}{2})^2 \pi^2 \alpha t / b^2} \cos(n+\frac{1}{2})\frac{\pi y}{b} \qquad (1)$$

where α is the thermal diffusivity coefficient of the material and the center of the slab is defined as y=0. Here, $\alpha = \kappa/(\rho \cdot C_P)$, where κ is the thermal conductivity of the material (W/m·K), ρ is the density of the material (kg/m^3), and C_p is the heat capacity (J/kg·K). Profiles computed using Equation 1 for different dimensionless times, t/τ, when immersing a slab with finite thickness and temperature $T=T_o$ in a hot reservoir having a temperature $T=T_1$ are shown in Figure 1. Here, τ is a characteristic time defined shortly.

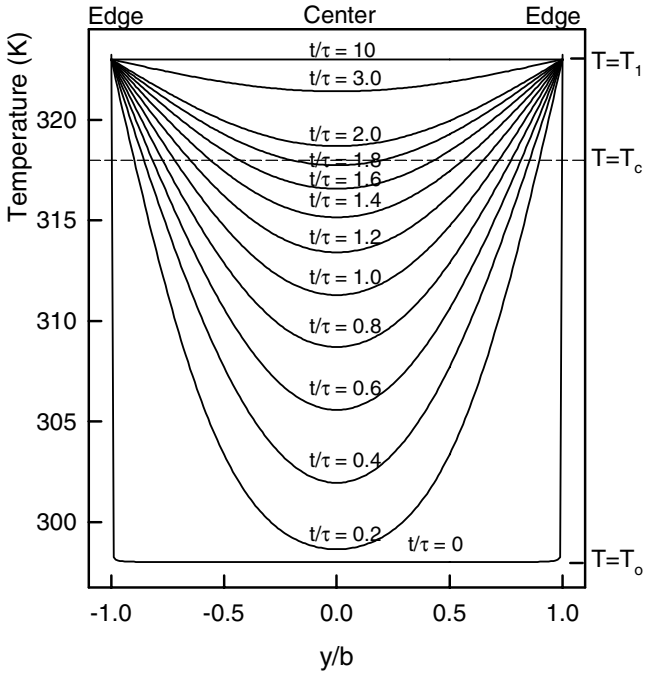

Figure 1. Temperature profile in a slab of finite thickness when immersed in a hot reservoir with temperature T_1. Sample initial temperature $T=T_o$, $T_1>T_o$, and sample thickness=$2b$.

For facile calculations, Equation 1 can be expanded and simplified to yield:

$$\frac{T_1 - T}{T_1 - T_0} = 2[\frac{2}{\pi} e^{-\frac{1}{4}\pi^2 \alpha t / b^2} \cos(\frac{\pi \cdot y}{2b}) - \frac{2}{3\pi} e^{-\frac{9}{4}\pi^2 \alpha t / b^2} \cos(\frac{3\pi \cdot y}{2b}) + \frac{2}{5\pi} e^{-\frac{25}{4}\pi^2 \alpha t / b^2} \cos(\frac{5\pi \cdot y}{2b}) - \ldots] \qquad (2)$$

In comparison to the first term (n=0), the second and higher terms are negligible, especially for longer times. Defining a dimensionless temperature $\theta(y,t)$ as $\theta(y,t) = \frac{T_1 - T(y,t)}{T_1 - T_0}$, and in light of the above simplification, the evolution of the slab's temperature profile with time will approximately follow:

$$\theta(y,t) = \cos(\frac{\pi \cdot y}{2b}) \cdot A \cdot e^{-t/\tau} , \tag{3}$$

where A is a pre-factor equal to $\frac{4}{\pi}$, and τ is a characteristic heat transfer time expressed as,

$$\tau = \frac{4}{\pi^2} \cdot \frac{b^2}{\alpha} . \tag{4}$$

Since the thermal diffusion coefficient, α, is proportional to the thermal conductivity,

$$\alpha = \kappa/\rho C_p \tag{5}$$

Equation 4 can be rewritten as

$$\tau = \frac{4}{\pi^2} \frac{\rho \cdot C_p}{\kappa} b^2 \tag{6}$$

where ρ is the bulk density (kg/m^3), C_p is the heat capacity (J/kg), κ is the thermal conductivity (W/m·K), and b is a characteristic dimension for transfer (m). Considering only the centerline (y=0) temperature, Equation 3 greatly simplifies to:

$$\theta(0,t) = A \cdot e^{-\frac{t}{\tau}} . \tag{7}$$

For a semi-infinite rectangular sample with width 2a and thickness 2b, which is a better approximation to the straight bars we tested hereafter, a two-dimensional heat transfer model needs to be considered. The solution can be modified from Equation 1,[4]

$$\theta(t) = \theta(x,t) \cdot \theta(y,t) \tag{8}$$

To be experimentally simple, we choose 2a=2b (i.e., a square cross-section), the characteristic heat transfer time yielded from Equation 8 is:

$$\tau = \frac{2}{\pi^2} \cdot \frac{b^2}{\alpha} \tag{9}$$

Equation 9 (two-dimensional heat transfer) differs from Equation 4 (one-dimensional heat transfer) only by a factor of 2; that is, the heat transfer speed doubles for the symmetric two-dimensional geometry.

Figure 1 and Equation 7 show that when immersed into a hot temperature reservoir, the slab's centerline temperature rises asymptotically with a characteristic rise time (Equation 7)

proportional to b^2 and inversely proportional to α. Hence, to decrease the heat transfer time and have the sample reach a targeted temperature as fast as possible, the slab should be as thin as possible, and the material thermal conductivity should be as high as possible. However, the first factor (sample dimension) is restricted, in most applications, due to the mechanical requirements or space limitations. Therefore, manipulation of the latter factor is critical. Since τ is the time required to heat the sample to a critical temperature in order to trigger the shape recovery, it will be referred to herein as *induction time*. We note that Figure 1 also reveals that the time for the center line of the slab to reach the critical temperature (depicted arbitrarily in this figure as $T=T_c$) is not necessarily equal to induction time τ, but different by a factor that is related to the initial slab temperature T_o, reservoir temperature T_1, and the critical transition temperature T_c. Thus, measurements of the shape memory induction time for various sample geometries cannot allow direct measurement of thermal conductivity.

EXPERIMENTAL DETAILS

Polycyclooctene having a high *trans* content (80%) (Vestenamer 8012®) was obtained from Degussa Corporation. The thermal initiator used to promote crosslinking was dicumyl peroxide (DCP), purchased from Aldrich Company. The boron nitride filler PT-140 (PolarTherm™) was purchased from GE Advanced Ceramic Corporation and the properties are listed in *Table 1*. All the materials were used as received.

Table 1. Properties of the BN filler per the vendor.

PolarTherm® Grade	PT-140
Surface Area (m^2/g)	7
Average Particle Size (μm)	9-12
Thermal Conductivity (W/m-K)	300+
Coeffcient of Linear Expansion, x 10^{-6}/°C	<1
Specific Heat (J/kg-K)	794
Theoretical Density (g/cm^3)	2.25

PCO was compounded with BN filler in a Brabender® batch mixer with a cavity volume of 30 ml. The mixer was first preheated to 80 ºC and equilibrated for at least 5 minutes to ensure a uniform temperature distribution within the whole chamber. The PCO pellets were first dry blended with DCP and BN powder to obtain the composition desired in the final products and then fed into the chamber over the course of 1 minute at a blade rotation speed of 25 rpm. This mixture was blended at 80 ºC for 10 minutes at the same rotation speed, followed which each mixture was then removed from the cavity and cooled to room temperature in air. The samples were then pressed between two hot plates preheated to 180 ºC and cured at this temperature for 30 minutes within a custom mold having the thickness of 3.5 mm under a load ≅ 8~9 metric ton (18000 lbs). The fully cured samples were then quenched to room temperature under load using the press cooling water, the load being released only after reaching room temperature. With careful handling, bubble free films with smooth surfaces were usually obtained by this method.

Thermal conductivity of the PCO and BN filled PCO composites were measured using an ASTM standard[5] as detailed in a previous publication.[2] The shape memory induction time

was measured using a cured and pre-stretched PCO and a PCO/20wt-% BN composite prepared using the same curing procedures. The samples were cut to a straight bar shape with a square cross section of varying lateral dimension. A square cross section was chosen since, for our samples, the heat transfer process is actually two-dimensional and the width-thickness ratio affects the induction time significantly as revealed in the Theory section. The sample bars were then pre-stretched to L_f = 200% in a tensile mode using a hot water bath at 50 °C. The stretched shape was then fixed by cooling in ice water. These samples were then loaded into a tensile fixture in a Perkin-Elmer DMA under small preload (0.02 N). The sample and the thermocouple were then promptly immersed into a hot water bath (not the Perkin-Elmer oven) at 50 °C to trigger shape recovery. Both the temperature and the shape recovery profiles were recorded and the induction time obtained by calculating the period between the onset of temperature increase and that of shape recovery, as shown schematically in Figure 2.

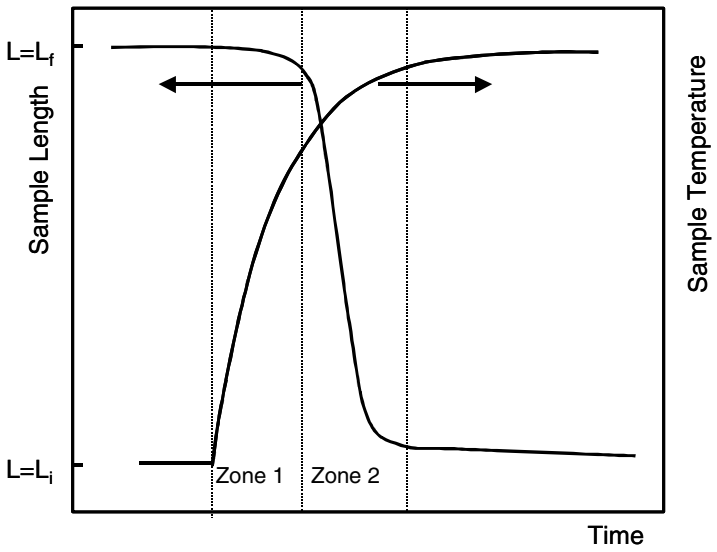

Figure 2. Schematic plot of the shape recovery profile when a prestretched and fixed sample is immersed into a hot medium to trigger the shape recovery. Zone 1 features heat transfer controlled by the sample geometry and thermal conductivity while Zone 2 features shape recovery controlled by the material's viscoelastic properties.

RESULTS AND DISCUSSION

The shape recovery of prestretched and chemically-crosslinked PCO and PCO/BN composites having the same crosslinking density and various cross-section was examined as described in Experimental Details. We found that with the decrease of the cross-sectional dimensions and the incorporation of thermal conducting filler, the overall shape recovery speed increases noticeably. Further analysis of the data revealed that two zones exist during the shape recovery process as indicated schematically in Figure 2: a thermal diffusion zone and a shape recovery zone. Data analysis revealed that the speeds of the shape recovery process, controlled by the viscoelastic properties of the material, do not vary obviously with the cross sectional dimensions, even for the case of 20% added BN (data not shown). This indicates that the major changes of the shape recovery speed are controlled by the heat transfer, manifested in Zone 1, as postulated.

The induction time data of chemically crosslinked PCO and BN reinforced PCO with the same crosslinking density were measured and are plotted versus the sample thickness (same as width, as measured before shape recovery) in a log-log plot in Figure 3. Our results show that with increasing sample thickness, the induction time increases considerably with a power law exponent near 2 (Equation 9) for both PCO and PCO/BN blend. Further, when the thermal conductivity was increased (nearly doubled) with added BN, the induction time decrease (to half) as predicted in the equation. The results are helpful for us to predict the shape recovery profiles and tailor the shape recovery properties using the present approach for thermal conductivity enhancement or others.

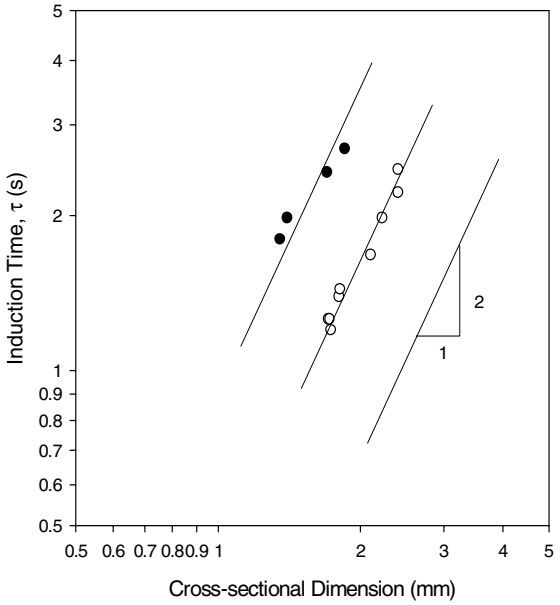

Figure 3. Shape recovery induction time versus sample cross-sectional dimension. Hot reservoir temperature $T_1 = 50 \pm 1$ °C, sample initial temperature $T_o = 25$ °C. All samples were chemically crosslinked with 1 wt% DCP. Solid circle: PCO; open circle: PCO:BN=80:20.

ACKNOWLEDGEMENTS

This research was supported by Boston Scientific Corporation.

[1] William D. Callister, Jr., *Material Science and Engineering: An Introduction*, 5th ed. (John Wiley & Son, Inc., New York, 2000) p. 808-809

[2] C. Liu and P. T. Mather, in *Annual Technical Conference - Society of Plastics Engineers (2004), May, 2004, Chicago IL*

[3] R. B. Bird; W. E. Stewart and E. N. Lightfoot; *Transport Phenomena,* (John Wiley & Sons Inc., New York, 1960) p. 354.

[4] H. S. Carslaw and J. C. Jaegen, *Conduction of Heat in Solid* 2nd ed. (Oxford University Press, Oxford, UK, 1960) p. 173.

[5] ASTM E 1952: 2001. *Standard Test Method for Thermal Conductivity and Thermal Diffusivity by Modulated Temperature Differential Scanning Calorimetry*. pp. 6.